frontiers | Frontiers in Neurology

Multi-Dimensional and Objective Assessment of Motion Sickness Susceptibility Based on Machine Learning

Cong-cong Li [1,2†], Zhuo-ru Zhang [1,3†], Yu-hui Liu [1,2†], Tao Zhang [4], Xu-tao Zhang [1,2*], Han Wang [1,2*] and Xiao-cheng Wang [1,2*]

[1] Center of Clinical Aerospace Medicine, School of Aerospace Medicine, Fourth Military Medical University, Xi'an, China, [2] Department of Aviation Medicine, The First Affiliated Hospital, Fourth Military Medical University, Xi'an, China, [3] Department of Pathophysiology, Medical College, Yan'an University, Yan'an, China, [4] Department of Medical Electronic Engineering, School of Biomedical Engineering, Fourth Military Medical University, Xi'an, China

Background: As human transportation, recreation, and production methods change, the impact of motion sickness (MS) on humans is becoming more prominent. The susceptibility of people to MS can be accurately assessed, which will allow ordinary people to choose comfortable transportation and entertainment and prevent people susceptible to MS from entering provocative environments. This is valuable for maintaining public health and the safety of tasks.

Objective: To develop an objective multi-dimensional MS susceptibility assessment model based on physiological indicators that objectively reflect the severity of MS and provide a reference for improving the existing MS susceptibility assessment methods.

Methods: MS was induced in 51 participants using the Coriolis acceleration stimulation. Some portable equipment were used to digitize the typical clinical manifestations of MS and explore the correlations between them and Graybiel's diagnostic criteria. Based on significant objective parameters and selected machine learning (ML) algorithms, several MS susceptibility assessment models were developed, and their performances were compared.

Results: Gastric electrical activity, facial skin color, skin temperature, and nystagmus are related to the severity of MS. Among the ML assessment models based on these variables, the support vector machine classifier had the best performance with an accuracy of 88.24%, sensitivity of 91.43%, and specificity of 81.25%.

Conclusion: The severity of symptoms and signs of MS can be objectively quantified using some indicators. Multi-dimensional and objective assessment models for MS susceptibility based on ML can be successfully established.

Keywords: motion sickness, susceptibility, objective assessment, machine learning, vestibular system

INTRODUCTION

Motion sickness (MS), as a response to exposure to a provocative environment, cannot essentially be called a disease. However, with the extension of activities from land and sea to the sky and outer space, the transformation of information sources from paper-based text and pictures to digital multimedia resources, and the increasing replacement of work by intelligent machines, MS has a greater effect on humans. MS has also evolved into several types, such as carsickness, seasickness, airsickness, space motion sickness, and visually induced motion sickness (VIMS), and there are not a few people who have experienced it (1–3). MS usually manifests as nausea, vomiting, pallor, cold sweat, drowsiness, headache, dizziness, and nystagmus; "Sopite syndrome" (4) and "Mal de debarquement syndrome (MdDS)" (5) are its special manifestations. At present, the pathogenesis of MS has not been fully elucidated, but the "sensory conflict theory," which revolves around the vestibular nervous system, is the most widely accepted (6). Research and exploration of the central mechanism proposed by this theory are ongoing (7).

Some scholars are keen to study why MS occurs, while others are more concerned with who is susceptible to MS and unable to work normally in provocative environments. Preventing the entry of people susceptible to MS into navigation, aviation, and aerospace occupations is important for maintaining the safety of tasks and the health of personnel. The assessment methods for the susceptibility to MS include tests in the actual environment, provocative tests, medical history surveys, psychological tendency tests, physiological tendency tests, and adaptation observations. Among them, provocative tests with a relatively high economy, safety, and accuracy are frequently used. Subjective rating scales for the severity of symptoms and signs of MS in participants have often been used in previous provocative tests; they include Graybiel's rating scales (8), Wiker's rating scales (9), and simulator sickness questionnaire (SSQ) for VIMS (10). These subjective evaluation methods are easy and convenient, but their accuracy is easily influenced by the motivation of the participant and the experience of the tester.

Hence, several scholars have begun research into various objective evaluation methods and indicators to assess the susceptibility of people to MS. Temperature (TEMP) (11), skin conductance level (SCL) (12), electrogastrography (EGG) (13), and heart rate variability (14) obtained solely from body surface recordings have a long history as objective indicators for assessing MS susceptibility, and Gavgani et al. found that SCL in the forehead was the best physiological correlate of VIMS-induced nausea symptoms (15). Objective assessments of MS susceptibility based on the results of vestibular function tests, such as the vestibulo-ocular reflex for different vestibular receptors (16–18), vestibular evoked myogenic potentials (19–21), and computerized dynamic posturography (22), are gradually becoming the focus of research, among them, the gain asymmetry of the video head impulse test, the nystagmus slow-phase velocity evoked by the caloric test and the amplitude of the cervical vestibular evoked myogenic potential vary in groups of participants with different susceptibility to MS. Functional brain assessments, such as electroencephalogram

(23, 24), functional magnetic resonance imaging (25, 26) and functional near-infrared spectroscopy (27, 28), have facilitated the objective assessment of MS susceptibility at the level of higher nerve centers, meanwhile, the correlation between the intensity of activity in certain brain regions during MS exposure and the degree of MS discomfort have been confirmed by several studies. In addition, the levels of arginine vasopressin, ghrelin and immunoglobulins in blood after MS exposure have been found to correlate with the severity of MS (29, 30), while the discovery of single-nucleotide polymorphism and chromosomes associated with MS susceptibility provides new alternatives for the assessment of MS susceptibility (31, 32). However, some of the methods and indicators mentioned above are not suitable for screening large populations, either because the equipment is not portable, or the testing environments are demanding, or invasive manipulations are required to obtain samples.

Thus, the aim of this study was to induce MS using a simple provocative stimulus and objectively quantify its typical manifestations of nausea, vomiting, pallor, cold sweat, dizziness, and nystagmus using portable instruments to explore the correlations between them and MS severity. Using significant objective parameters and several machine learning (ML) algorithms, multi-dimensional and objective MS susceptibility assessment models were developed, and their performances were compared to provide a reference for improving the existing MS susceptibility assessment methods.

MATERIALS AND METHODS

Participants

In order to obtain objective indicators related to the severity of MS, sample size estimation for Pearson correlation analyses were performed using PASS 15 (NCSS Statistical Software, USA), with a threshold of $p = 0.05$, a power of 0.9, and a predicted correlation coefficient between 0.4 and 0.6, yielding a sample size N between 24 and 61. The trial recruited 51 male participants (mean age, 24.54 ± 3.19 years; mean height 175.25 ± 5.80 cm; mean weight, 71.54 ± 2.89 kg), and none of them had a history of epilepsy, increased intracranial pressure, vertigo, cerebrovascular accident, severe mental illness, and drug abuse. None of the participants took any medications or alcoholic beverages within 48 h, and they participated in the experiment 1 h after eating. Physical examination of each participant showed no signs of external otitis, tympanic membrane perforation, or spontaneous nystagmus. Their naked or corrected visual acuity were 1.0 at least and color vision were normal. The study was approved by the Ethics Committee of the First Affiliated Hospital of the Fourth Military Medical University (number: KY-20202054-F-2). Each participant signed an informed consent form and volunteered to participate.

Equipment and Materials

An electric rotating chair (VTS-0, Peace, China) and Coriolis acceleration stimulation were used to induce MS. The videonystagmography (VNG) equipment (YD-III, Isen, China) fixed on the back of the electric rotating chair was used to record the nystagmus of each participant after the electric rotating chair

stopped suddenly. The wireless physiological signal acquisition and analysis system (PhysioLab, Ergoneers, Germany) has multiple sensor channels, such as those for TEMP, SCL, and EGG, and can display and record data in real-time on a computer via Bluetooth. A portable colorimeter (TS7600, 3 nh, China) can be held by one hand to collect skin color parameters, and the skin color can be digitized through the CIE-L*a*b* color system (33). A posturography equipment (Balance-A, Nuocheng, China) was located next to the electric rotating chair and can be used to quickly assess the equilibrium of the participant. Graybiel's rating scale was used to assess the severity of MS in participants.

Procedure

All tests were carried out in a laboratory with no airflow but automatic light adjustment, and the room temperature was between 20 and 26°C. After reaching the laboratory, each participant took a 30-min break to acclimatize to the test environment. During this period, the participants were shown the movements that produced the Coriolis acceleration stimulation and were requested to truthfully describe their subjective feelings during the test. Considering the late-onset effect of the vestibulo-autonomic response, the entire test was divided into three phases: 10 min for Pre-exposure (pre-E), 90 s of exposure (E), and 30 min for Post-exposure (post-E) to Coriolis acceleration stimulation (**Figure 1**). The MS of the participants was induced by sitting on a rotating chair at an angular speed of 180°/s for 90 s, during which their heads were swung from a 30° leftward tilt to a 30° rightward tilt (from a 30° rightward tilt to a 30° leftward tilt) once every 2 s.

Data Acquisition and Processing

Experimental data were obtained by various instruments through continuous recording or acquisition at specific time points, and the data acquisition methods are presented in **Figure 1**. Skin temperature ($TEMP_S$), SCL, and EGG signals were recorded continuously at a sampling frequency of 1 kHz throughout the experiment. VNG data were collected at a sampling frequency of 30 Hz after the emergency stopping of the rotating chair and with the eyes of the participant open. CIE-L*a*b* data were obtained by measuring the skin color of the left and right cheeks of the participant, and five measurements were taken during the pre- and post-E periods (**Figure 1**). The equilibrium data were collected with the eyes of the participant closed 10 min before and 10 min after exposure to Coriolis acceleration stimulation. Graybiel's rating scales were used four times during the post-E period (**Figure 1**), and the severity of MS was assessed for seven components, including nausea syndrome, skin color, cold sweat, salivation, drowsiness, pain, and central nervous system abnormalities.

TEMPs and SCL were obtained from PhysioLab 2021 (Ergoneers, Germany) for exact values. The EGG of nausea and vomiting in MS is mainly characterized by 4–10 cycles per min (cpm) of stomach electrical activity increase (34), and this irregular activity was defined as tachyarrhythmia. Therefore, for the EGG signal, we applied a high-pass filter with a cut-off frequency of 0.067 Hz and a low-pass filter with a cut-off frequency of 0.167 Hz using EDF browser 1.56
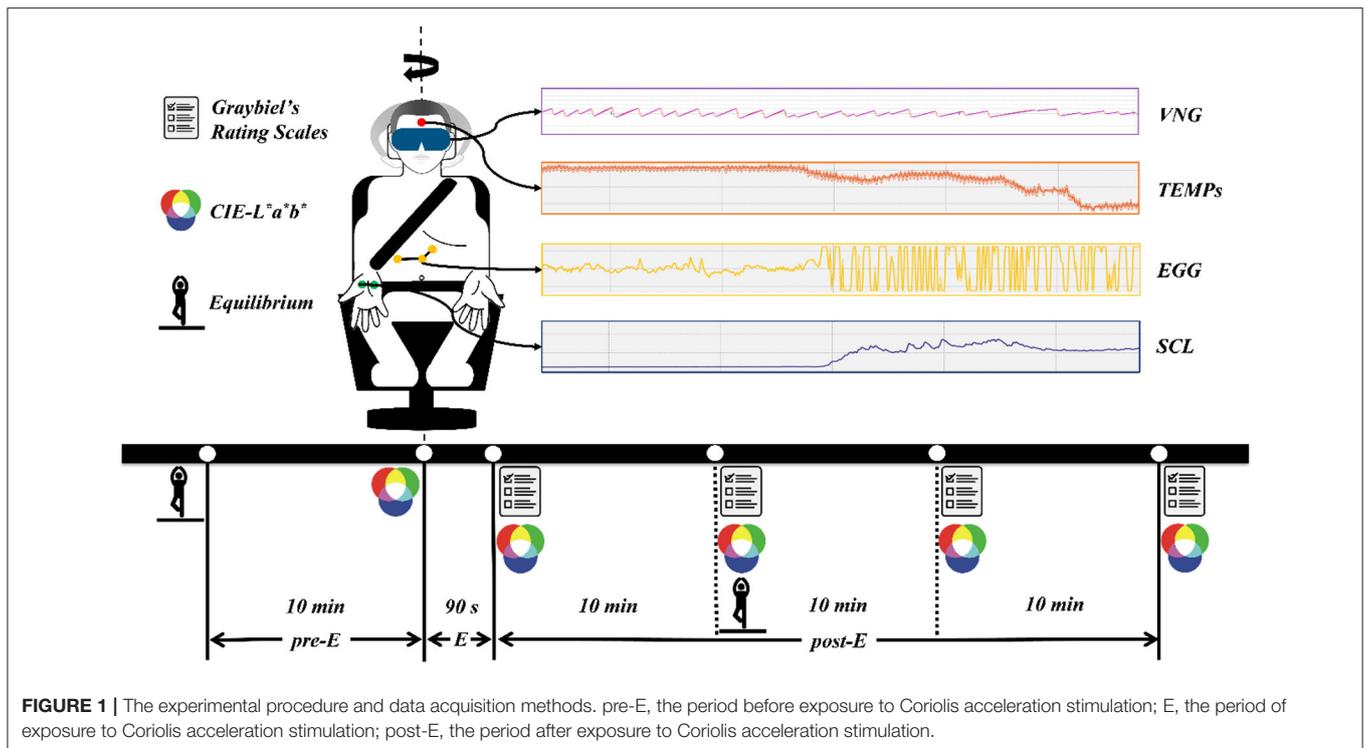
(open-source software) and performed a frequency domain analysis of the 0.067–0.167 Hz band to obtain the amplitude ($AMP_{EGG0.067-0.167}$) and power ($POW_{EGG0.067-0.167}$) of the EGG signal in this band. We used the ISEN-VNG 2.1 (ISEN, China) to select three maximal slow-phase velocities (MSPVs) for each VNG, and their average value ($MSPV_{L-R}$) was used for analysis. In the CIE-L*a*b* color system, the CIE-L* value indicates that the color changes from black to white, the CIE-a* value indicates that the color changes from green to red, and the CIE-b* value indicates that the color changes from blue to yellow (33). Hence, CIE-L* and CIE-a* values were chosen to assess the pallor at the onset of MS and were analyzed using the average of the left and right cheek measurements ($CIE-L^*_{L-R}$, $CIE-a^*_{L-R}$). The equilibrium of the participants was assessed primarily by measuring their total traveled way (TTW) and envelope area (EA) of the center of pressure. Graybiel's rating scales were applied by the same senior otolaryngologist, and the sum of the maximum values of the seven dimensions of these rating scales at each specific time point was obtained as Graybiel's $score_{max}$.

Statistical Analysis

The statistical analyses of the data in this study had the following three steps. (1) First, objective indicators that showed significant changes before and after exposure to MS were determined. The $AMP_{EGG0.067-0.167}$ and $POW_{EGG0.067-0.167}$ data were taken as the baseline for 10 min of the pre-E period and as control for the first 10 min of the post-E period. The TEMPs, SCL, CIE-L^*_{L-R}, and CIE-a^*_{L-R} were compared using the extreme values measured before and after the Coriolis acceleration stimulation. The TTW and EA were compared before and after the Coriolis acceleration stimulation. A paired t-test was used to analyze the differences in each objective indicator. (2) Second, objective indicators that changed significantly before and after exposure to MS and whose variations correlated with the severity of MS were screened. Two-tailed Pearson's correlation analyses were carried out for the change in the objective indicators selected in step 1 and the Graybiel's $score_{max}$. $MSPV_{L-R}$ was also analyzed for Pearson's correlation with the Graybiel's $score_{max}$. (3) Several assessment models of MS susceptibility based on ML were established. We used the variations of the objective indicators selected in step 2 as input variables; "Graybiel's $score_{max} \geq 5$" as the output indicating "susceptible to MS" and "Graybiel's $score_{max} < 5$" as the output indicating "not susceptible to MS" (35), to develop MS susceptibility assessment models by using different ML algorithms. We also compared the performances of the models. Statistical analyses and charting were performed using SPSS 22.0 (IBM Corporation, USA), GraphPad Prism 8.0 (GraphPad Software, USA), and Origin 2018 (OriginLab Corporation, USA). Statistical significance was set at $p < 0.05$.

ML Algorithms and Tools

In this study, four widely applied ML algorithms, including support vector machine (SVM), random forest (RF), K-nearest neighbor (KNN), and multilayer perceptron (MLP), were used to build the assessment models of MS susceptibility. SVM separates different types of data points by drawing a virtual hyperplane and is widely used for small sample data (36). RF is an integrated

FIGURE 1 | The experimental procedure and data acquisition methods. pre-E, the period before exposure to Coriolis acceleration stimulation; E, the period of exposure to Coriolis acceleration stimulation; post-E, the period after exposure to Coriolis acceleration stimulation.

classifier consisting of several randomly generated decision tree classifiers, which has a better classification performance than traditional decision tree algorithms (37). KNN finds the k-nearest training samples to the test samples based on a distance measure and uses the information of these k "neighbors" to classify the test samples (38). As a feedforward artificial neural network, MLP can be used to construct effective classifier algorithms to distinguish Non-linear separable data (39).

We used the Scikit-learn ML algorithm package based on Python 3.7 to build the above four classifiers (40), and the performances of these models were compared. On the one hand, we selected 70% of the 51 samples as the training set and 30% as the test set for dichotomous classification of MS susceptibility, and we performed a stratified random sampling according to the proportion of participants "susceptible to MS" and "not susceptible to MS" when selecting data for the training and test sets. The receiver operator characteristic curve (ROC) and area under the ROC (AUC) of each classifier were obtained. The above processes were repeated 100 times to obtain the respective average AUCs of the four models. In contrast, a 10-fold cross-validation was performed on the 51 samples to compare the accuracy, sensitivity, specificity, positive predictive value (precision), and negative predictive value of the four models.

RESULTS

All 51 participants successfully completed the experiment following the procedure and honestly reported various physical discomforts at different time points after exposure to MS. After
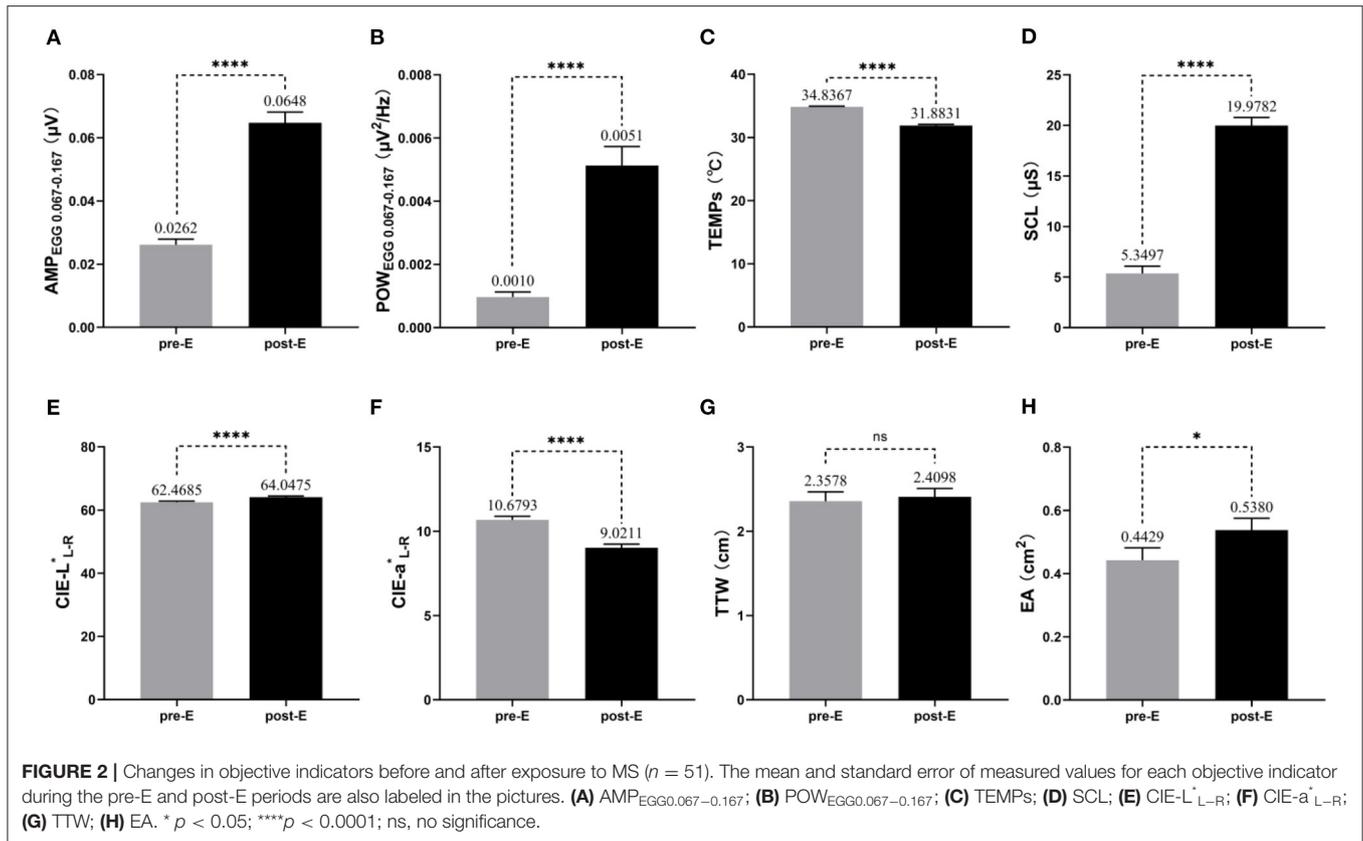
processing and statistical analyses of all experimental data, the following results were obtained.

Effects of the Coriolis Acceleration Stimulation on Objective Indicators

As shown in **Figure 2**, compared to the baseline before exposure, most of the objective indicators we focused on changed visually after exposure to Coriolis acceleration stimulation. Paired t-tests showed that $AMP_{EGG0.067-0.167}$, $POW_{EGG0.067-0.167}$, SCL, CIE-L^*_{L-R}, and EA increased significantly ($t = 12.27$, $p < 0.0001$ for $AMP_{EGG0.067-0.167}$, **Figure 2A**; $t = 7.151$, $p < 0.0001$ for $POW_{EGG0.067-0.167}$, **Figure 2B**; $t = 17.77$, $p < 0.0001$ for SCL, **Figure 2D**; $t = 12.05$, $p < 0.0001$ for CIE-L^*_{L-R}, **Figure 2E**; $t = 2.451$, $p = 0.0178$ for EA, **Figure 2H**), while TEMPs and CIE-a^*_{L-R} decreased significantly ($t = 17.02$, $p < 0.0001$ for TEMPs, **Figure 2C**; $t = 14.03$, $p < 0.0001$ for CIE-a^*_{L-R}, **Figure 2F**), but TTW did not change remarkably ($t = 0.6095$, $p = 0.5449$, **Figure 2G**). The trend of changes in the above objective indicators was consistent with the typical signs and symptoms of MS.

Objective Indicators That Can Reflect the Severity of MS

Because TTW did not change significantly before and after Coriolis acceleration stimulation, it was not included in the correlation analyses with Graybiel's score$_{max}$, which represents the severity of MS. Given the exponential increase in the EGG-related indicators, we obtained the logarithmic values of multiples of change in $AMPEGG_{0.067-0.167}$ and $POW_{EGG0.067-0.167}$ ($LOG\Delta AMP_{EGG0.067-0.167}$ and

FIGURE 2 | Changes in objective indicators before and after exposure to MS ($n = 51$). The mean and standard error of measured values for each objective indicator during the pre-E and post-E periods are also labeled in the pictures. **(A)** $AMP_{EGG0.067-0.167}$; **(B)** $POW_{EGG0.067-0.167}$; **(C)** TEMPs; **(D)** SCL; **(E)** CIE-L$^*_{L-R}$; **(F)** CIE-a$^*_{L-R}$; **(G)** TTW; **(H)** EA. $^* p < 0.05$; $^{****} p < 0.0001$; ns, no significance.

$LOG\Delta POW_{EGG0.067-0.167}$), with the change in the values of other meaningful objective indicators and $MSPV_{L-R}$, for Pearson's correlation analyses with Graybiel's score$_{max}$. For $LOG\Delta AMP_{EGG0.067-0.167}$ (**Figure 3A**), the correlation with Graybiel's score$_{max}$ was significant ($r = 0.3656$, $p = 0.0083$). Also significantly correlated with Graybiel's score$_{max}$ were $LOG\Delta POW_{EGG0.067-0.167}$ ($r = 0.4920$, $p = 0.0002$, **Figure 3B**), $\Delta TEMPs$ ($r = 0.5473$, $p < 0.0001$, **Figure 3C**), $MSPV_{L-R}$ ($r = 0.3817$, $p = 0.0058$, **Figure 3D**), ΔCIE-L$^*_{L-R}$ ($r = 0.4900$, $p = 0.0003$, **Figure 3E**), and ΔCIE-a$^*_{L-R}$ ($r = 0.5493$, $p < 0.0001$, **Figure 3F**). As a result, the above 6 variables could objectively represent the severity of MS in some degree. However, no significant correlation was found between ΔSCL and Graybiel's score$_{max}$ ($r = 0.2009$, $p = 0.1574$), as well as ΔEA ($r = -0.1392$, $p = 0.3302$).

ML Classifiers and Their Performance Comparison

The SVM, RF, KNN, and MLP classifiers for MS susceptibility were based on the above 6 variables related to the severity of MS. The means and standard deviations of the AUC values of the four models were obtained by training and testing with 100 stratified random samples (**Table 1**), and the difference between the AUC values of the groups was confirmed by the Kruskal-Wallis test and Dunn's multiple comparisons test (**Figure 4**). Among the four models, the SVM classifier had the best performance, with the

highest average AUC value (0.8795 ± 0.0815) for 100 times of classification training and testing.

We also presented the classification results of the 10-fold cross-validation of the four models for 51 samples using a confusion matrix (**Figure 5**) and compared the performances of the ML classifiers (**Table 2** and **Figure 6**). As can be seen, also, SVM classifier performed well with an accuracy of 88.24%, sensitivity of 91.43%, specificity of 81.25% and AUC value of 0.8634 for predicting MS susceptibility. In general, the classification results of SVM classifier were the most satisfactory.

DISCUSSION

For the general public, an objective and accurate understanding of their susceptibility to MS can help them choose more comfortable means of transportation and recreation and actively prevent the adverse effects of MS. However, for people working in special environments, such as drivers, astronauts, pilots, sailors, divers, extreme sports personnel, and operators of unmanned equipment or simulators, exposure to provocative motion environments is usually inevitable. Therefore, it is worthwhile to reduce the influence of human subjective factors and implement an objective and accurate assessment of the susceptibility to MS in those who are ready to join the above-mentioned special jobs.

Our study induced MS with the normative Coriolis acceleration stimulus and objectively quantified the typical manifestations of MS, such as nausea, vomiting, pallor, cold
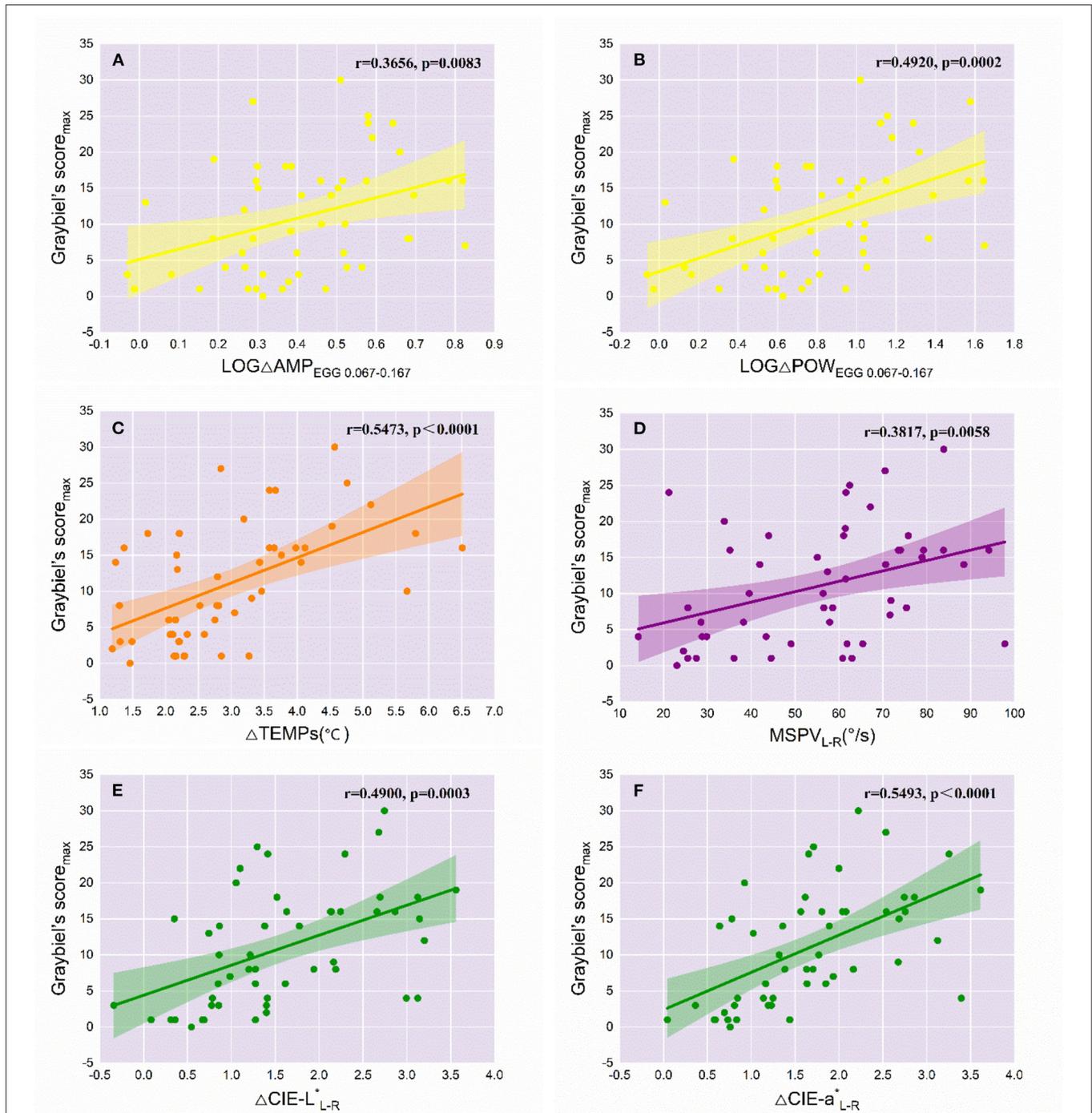
FIGURE 3 | Correlations of the variations of objective indicators with the severity of MS ($n = 51$). The r and p values of the objective variables significantly correlated with Graybiel's score$_{max}$ are labeled in each graph. The colored line represents the line of best fit for each linear regression, while the shaded area indicates the 95% confidence interval. **(A)** LOG$\triangle$AMP$_{EGG0.067-0.167}$; **(B)** LOG$\triangle$POW$_{EGG0.067-0.167}$; **(C)** $\triangle$TEMPs; **(D)** MSPV$_{L-R}$; **(E)** $\triangle$CIE-L$^*_{L-R}$; **(F)** $\triangle$CIE-a$^*_{L-R}$.
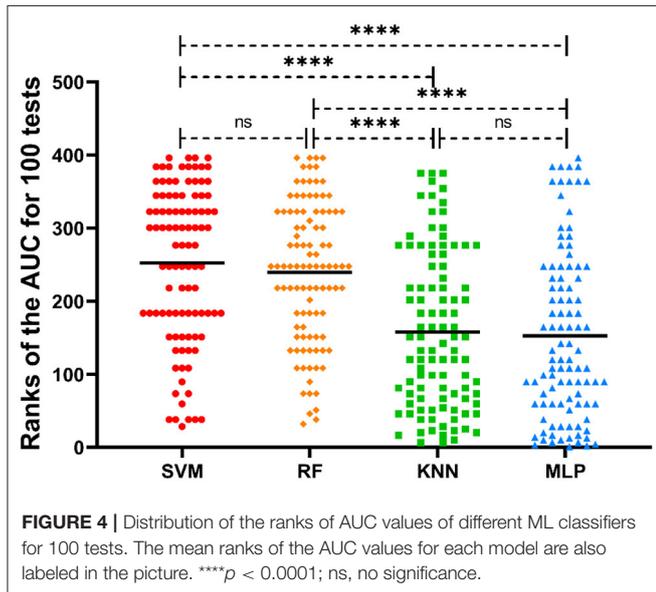
sweat, dizziness, and nystagmus, using a reproducible approach. We successfully sieved out several parameters related to gastric electrical activity, facial skin color, skin temperature, and nystagmus that could objectively assess the severity of MS, and these findings are similar to the results of previous studies.

Chinese scholars also used Coriolis acceleration stimulation to induce MS and found that the tachyarrhythmia of EGG was significantly enhanced in participants with severe MS (41), but they only compared EEG differences between groups with different levels of MS; Gruden et al. used a vehicle simulator

TABLE 1 | Means and standard deviations of AUC for 100 tests of the ML classifier.

Classifier	Mean	Standard deviation
SVM	**0.8795**	**0.0815**
RF	0.8703	0.0716
KNN	0.8007	0.0925
MLP	0.7904	0.1113

The bold values indicate that the SVM classifier had the best performance among the four models.

FIGURE 4 | Distribution of the ranks of AUC values of different ML classifiers for 100 tests. The mean ranks of the AUC values for each model are also labeled in the picture. ****$p < 0.0001$; ns, no significance.

to induce VIMS and found that the magnitude and duration of elevated EGG signals in participants correlated with their subjective level of nausea (42), but they used the SSQ scales, which are more suitable for VIMS, as the reference for correlation analyses. It has been reported that the magnitude of reduction in TEMP correlates with the degree of subjective discomfort induced by different levels of MS (43), a study on the treatment of MS consistently showed the efficacy of "promethazine + dextroamphetamine" in reducing MS symptoms and preventing a core temperature drop (44), but these studies also only compared the magnitude of TEMP decrease between groups with different levels of MS or with different anti-MS drugs. Both the MSPV of vestibulo-ocular reflex induced by the caloric test and the rotating chair test have been proven to be associated with susceptibility to MS (18, 45), however, neither of the related studies was grouped by severity of MS after the Coriolis acceleration stimulation. By contrast, our selected objective indicators better achieved a linear quantitative assessment of the severity of MS. In particular, to the best of our knowledge, our study is the first to assess the severity of MS by objectively measuring skin color.

Meanwhile, we did not find a significant correlation between the severity of MS and the changes in SCL, TTW, and EA,

which is not consistent with the reports of previous studies. When Gavgani et al. studied VIMS, they found that SCL of the fingers was significantly correlated with the degree of nausea, but they only classified nausea as one symptom of MS into four levels to analyze the data (15), unlike in the current study that correlated the changes in skin SCL with the exact scores of Graybiel's rating scales, and the difference between the two results was acceptable. Moreover, various physiological and psychological changes such as excitement, anger, fear, agitation, and fatigue can cause fluctuations in skin SCL, which is also sensitive to variations in external elements such as temperature, humidity, air flow, and clothing; therefore, it is challenging to objectively and accurately assess the severity of MS using SCL as the only indicator. In addition, the possible reasons for the insignificant correlations between the changes in TTW and EA and the severity of MS in this study are as follows. (1) First, to prevent the effect of body movement on the accuracy of other physiological parameters collected, we performed the second equilibrium test 10 min after the Coriolis acceleration stimulation; the long period for recovery may have mildened the symptoms of dizziness and instability in MS susceptible persons. (2) Since the participants were not familiarized with the method for equilibrium measurement before the test, the training effect may have also affected the test results. Further studies are needed to verify whether optimizing the experimental design will result in new findings.

Previous studies have focused on the screening of physiological markers that can objectively evaluate MS and VIMS, and ML modeling for MS susceptibility assessment has mostly targeted VIMS (25, 46, 47). In this study, we induced MS with real vestibular stimuli, as well as pioneered the collection of objective physiological parameters from multiple dimensions simultaneously, and the use of various ML methods to establish the optimal model for MS susceptibility assessment. According to the experimental results, the assessment model based on the SVM was optimal because of its relatively high sensitivity and specificity, which facilitates not only the identification of people susceptible to MS but also, and more importantly, the selection of people who are not susceptible to MS for special jobs where they are frequently exposed to provocative motion environments.

The pathogenesis of MS has not yet been fully elucidated. However, according to the classical "sensory conflict theory" of MS, all types of sensory conflicts that cause MS do not lack the information input from the vestibular system (6). The vestibular nuclei, as a repeater of vestibular information input and efferent, have extensive fiber connections with vision, proprioception, and other brain nuclei (48), and the susceptibility to MS is reduced in those with vestibular loss or hypofunction (49). Thus, it is reasonable to believe that the functional state of the vestibular system plays a crucial role in the onset and development of MS, and many clinical manifestations of MS are exported through different vestibular pathways. Based on this, we selected objective indicators that can be easily quantified in the vestibular pathway for the experiment, such as EGG, TEMPs, SCL, CIE-L*, and CIE-a* in the vestibulo-autonomic pathway, MSPV in the vestibulo-ocular pathway, and TTW and EA in the vestibulo-spinal pathway. We were pleased to find that

FIGURE 5 | Confusion matrix for the classification results of different classifiers.
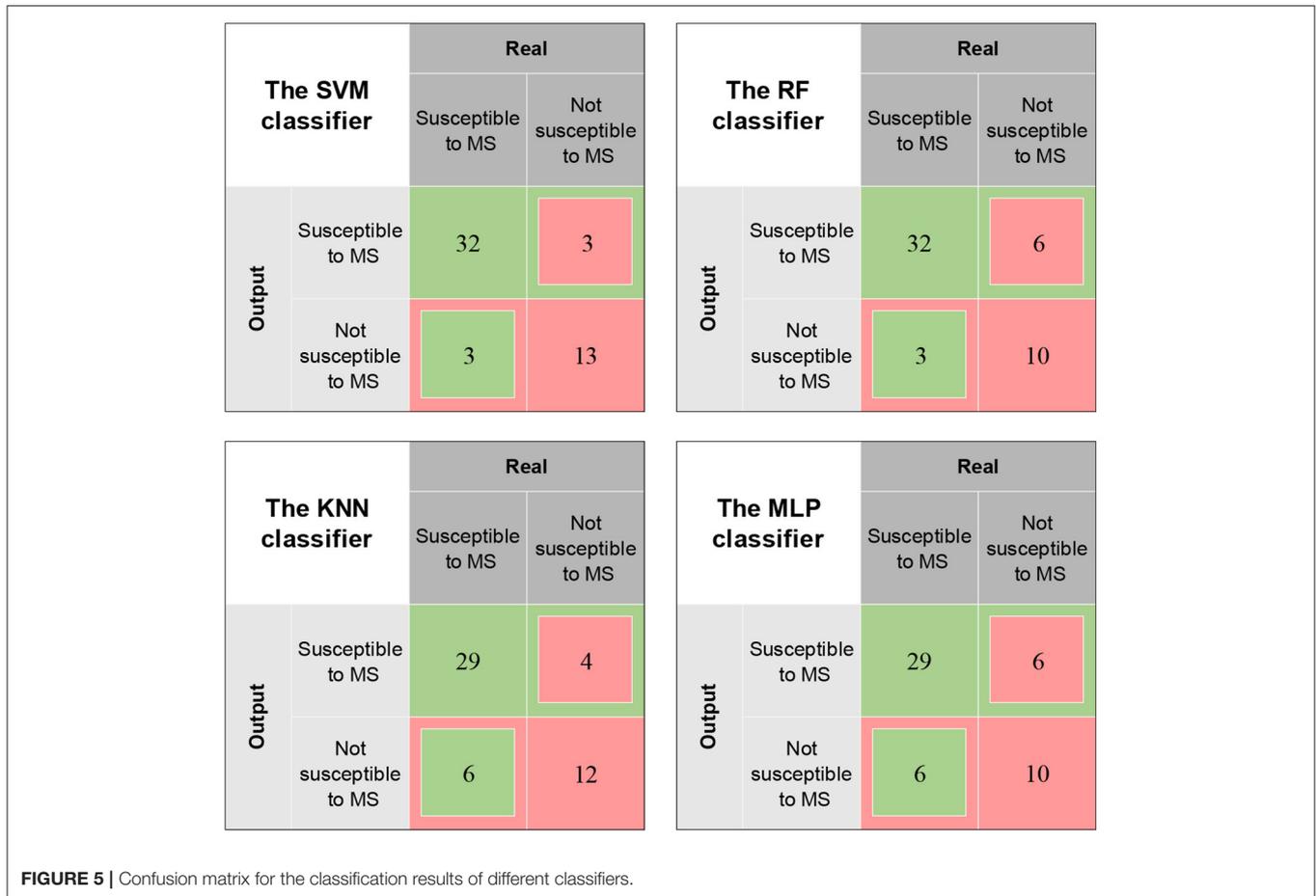
TABLE 2 | Evaluation of the performances of different ML classifiers.

Classifier	Accuracy	Sensitivity	Specificity	Positive predictive value (precision)	Negative predictive value
SVM	**0.8824**	**0.9143**	**0.8125**	**0.9143**	**0.8125**
RF	0.8236	0.9143	0.6250	0.8421	0.7692
KNN	0.8039	0.8286	0.7500	0.8789	0.6667
MLP	0.7647	0.8286	0.6250	0.8286	0.6250

The bold values indicate that the SVM classifier had the best performance among the four models.

participants with a mild MS response to the same intensity of provocative vestibular stimulus showed relatively small changes in the magnitude of the objective indicators, and the subjective severity of MS correlated well with the objective output based on the vestibular pathways. However, people with mild MS are able to maintain body balance and perform spatial orientation normally, just as their vestibular system is stable and does not overreact to external provocative stimuli. This is comparable to the normal immune system, which can resist pathogens and maintain health without overly reacting to antigens and causing allergic reactions or autoimmune diseases. From this perspective, the assessment of MS susceptibility is similar to performing a skin (or intradermal) sensitivity test, but the skin (or intradermal) sensitivity test has its own standard operating

procedure and objective method for judging the result, which is what we want to do with the assessment of MS susceptibility. Furthermore, with the deepening of basic research on MS, as well as the upgrading of smart wear and artificial intelligence, we hope that our study will provide a reference for the accurate assessment of MS susceptibility, the real-time monitoring of MS, and the development of integrated equipment for "examination-training-assessment" of vestibular function stability to facilitate the prevention and optimal treatment of MS.

LIMITATIONS

Our study has limitations, such as the timing of the acquisition of equilibrium parameters and training effects mentioned in the

FIGURE 6 | Comparison of the ROC curves of different ML classifiers. The SVM classifier performs best.
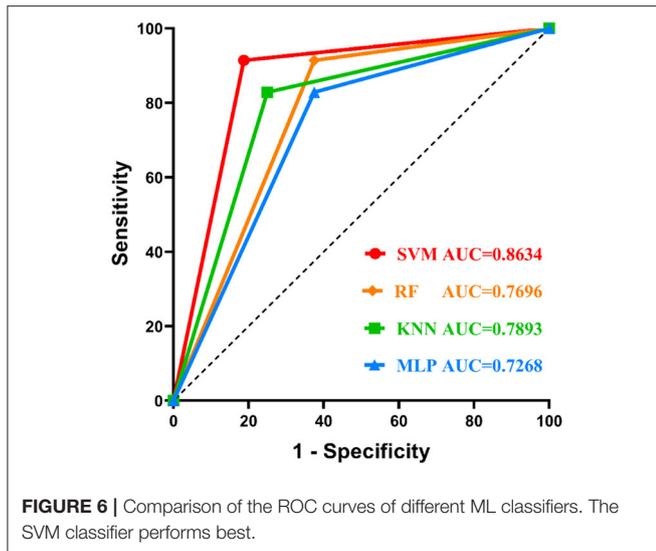
previous discussion section. It is difficult to precisely regulate temperature and humidity in the laboratory, as well as shield against noise, which may have led to errors in the experimental data. Finally, the sample of our study was not large enough, which may have limited the performance of various ML algorithms for the model and impacted the stability of the evaluation model.

CONCLUSION

This study induced MS using a uniform Coriolis acceleration stimulus and obtained some indicators related to gastric electrical activity, facial skin color, skin temperature, and nystagmus, which could be used to objectively and quantitatively assess the severity of MS. Based on these, several assessment models

based on different ML algorithms were developed and compared, among which, the SVM model with the best performance could be suitable for a multi-dimensional objective assessment of MS susceptibility.

DATA AVAILABILITY STATEMENT

The raw data supporting the conclusions of this article will be made available by the authors, without undue reservation.

ETHICS STATEMENT

The studies involving human participants were reviewed and approved by the Ethics Committee of The First Affiliated Hospital of the Fourth Military Medical University. The patients/participants provided their written informed consent to participate in this study.

AUTHOR CONTRIBUTIONS

C-cL, Y-hL, X-tZ, and X-cW conceived and designed the experiment methods. C-cL, Z-rZ, Y-hL, and X-cW organized experiments and collected relevant data. C-cL, Z-rZ, TZ, and HW conducted the statistics and machine learning modeling. C-cL, Z-rZ, Y-hL, and TZ drafted the manuscript. X-tZ, HW, and X-cW revised the manuscript. All authors take responsibility for the integrity of the data and the accuracy of data analysis. All authors contributed to the article and approved the submitted version.

FUNDING

REFERENCES

1. Turner M, Griffin MJ, Holland I. Airsickness and aircraft motion during short-haul flights. *Aviat Space Environ Med.* (2000) 71:1181–9. doi: 10.1053/apmr.2000.20625

2. Schmidt EA, Kuiper OX, Wolter S, Diels C, Bos JE. An international survey on the incidence and modulating factors of carsickness. *Transport Res.* (2020) 71:76–87. doi: 10.1016/j.trf.2020.03.012

3. Sharples S, Cobb S, Moody A, Wilson JR. Virtual reality induced symptoms and effects (VRISE): comparison of head mounted display (HMD), desktop and projection display systems. *Displays.* (2008) 29:58–69. doi: 10.1016/j.displa.2007.09.005

4. Foster M, Singh N, Kwok K, Macefield VG. Vestibular modulation of skin sympathetic nerve activity in sopite syndrome induced by low-frequency sinusoidal motion. *J Neurophysiol.* (2020) 124:1551–9. doi: 10.1152/jn.00177.2020

5. Chen Y, Tang JH, Shou G, Gleghorn D, Doudican BC, Besio W, et al. Effect of body positions on EEG signals in mal de debarquement syndrome. *Annu Int Conf IEEE Eng Med Biol Soc.* (2018) 2018:1931–4. doi: 10.1109/EMBC.2018.8512699

6. Koch A, Cascorbi I, Westhofen M, Dafotakis M, Klapa S, Kuhtz-Buschbeck JP. The neurophysiology and treatment of motion sickness. *Dtsch Arztebl Int.* (2018) 115:687–96. doi: 10.3238/arztebl.2018.0687

7. Cohen B, Dai M, Yakushin SB, Cho C. The neural basis of motion sickness. *J Neurophysiol.* (2019) 121:973–82. doi: 10.1152/jn.00674.2018

8. Graybiel A, Wood CD, Miller EF, Cramer DB. Diagnostic criteria for grading the severity of acute motion sickness. *Aerosp Med.* (1968) 39:453–5.

9. Wiker SF, Kennedy RS, McCauley ME, Pepper RL. Susceptibility to seasickness: influence of hull design and steaming direction. *Aviat Space Environ Med.* (1979) 50:1046–51.

10. Kennedy RS, Lane NE, Berbaum KS, Lilienthal MG. Simulator sickness questionnaire: an enhanced method for quantifying simulator sickness. *Int J Aviat Psychol.* (1993) 3:203–20. doi: 10.1207/s15327108ijap0303_3

11. Nalivaiko E, Rudd JA, So RH. Motion sickness, nausea and thermoregulation: the "toxic" hypothesis. *Temperature.* (2014) 1:164–71. doi: 10.4161/23328940.2014.982047

12. Warwick-Evans L, Church R, Hancock C, Jochim D, Ward F. Electrodermal activity as an index of motion sickness. *Aviat Space Environ Med.* (1987) 58:417–23.

13. Cheung B, Vaitkus P. Perspectives of electrogastrography and motion sickness. *Brain Res Bull.* (1998) 47:421–31. doi: 10.1016/S0361-9230(98)00095-1

14. Wang JQ, Qi RR, Pan LL, Zhou W, Zhang LL, Cai YL. Motion sickness and resting energy expenditure in Chinese male adults. *Aerosp Med Hum Perform.* (2016) 87:360–6. doi: 10.3357/AMHP.4438.2016

15. Gavgani AM, Nesbitt KV, Blackmore KL, Nalivaiko E. Profiling subjective symptoms and autonomic changes associated with cybersickness. *Auton Neurosci.* (2017) 203:41–50. doi: 10.1016/j.autneu.2016.12.004

16. Neupane AK, Gururaj K, Sinha SK. Higher asymmetry ratio and refixation saccades in individuals with motion sickness. *J Am Acad Audiol.* (2018) 29:175–86. doi: 10.3766/jaaa.16175

17. Kitajima N, Sugita-Kitajima A. Ocular counter-rolling in scuba divers with motion sickness. *Auris Nasus Larynx.* (2021) 48:214–20. doi: 10.1016/j.anl.2020.08.007

18. Fowler CG, Dallapiazza M, Hadsell KT. Vestibular function and motion sickness susceptibility: videonystagmographic evidence from oculomotor and caloric tests. *Am J Audiol.* (2020) 29:188–98. doi: 10.1044/2020_AJA-19-00050

19. Singh NK, Pandey P, Mahesh S. Assessment of otolith function using cervical and ocular vestibular evoked myogenic potentials in individuals with motion sickness. *Ergonomics.* (2014) 57:1907–18. doi: 10.1080/00140139.2014.952683

20. Fowler CG, Sweet A, Steffel E. Effects of motion sickness severity on the vestibular-evoked myogenic potentials. *J Am Acad Audiol.* (2014) 25:814–22. doi: 10.3766/jaaa.25.9.4

21. Xie SJ, Chen W, Jia HB, Wang ZJ, Yao Q, Jiang YY. Ocular vestibular evoked myogenic potentials and motion sickness susceptibility. *Aviat Space Environ Med.* (2012) 83:14–8. doi: 10.3357/ASEM.3101.2012

22. Alharbi AA, Johnson EG, Albalwi AA, Daher NS, Cordett TK, Ambode OI, et al. Effect of visual input on postural stability in young adults with chronic motion sensitivity: a controlled cross-sectional study. *J Vestib Res.* (2017) 27:225–31. doi: 10.3233/VES-170534

23. Guofa S, Han Y, Urbano D, Yoon-Hee C, Lei D. Changes of symptom and EEG in mal de debarquement syndrome patients after repetitive transcranial magnetic stimulation over bilateral prefrontal cortex: a pilot study. *Annu Int Conf IEEE Eng Med Biol Soc.* (2014) 2014:4294–7. doi: 10.1109/EMBC.2014.6944574

24. Chuang SW, Chuang CH, Yu YH, King JT, Lin CT. EEG alpha and gamma modulators mediate motion sickness-related spectral responses. *Int J Neural Syst.* (2016) 26:1650007. doi: 10.1142/S0129065716500076

25. Ruffle JK, Patel A, Giampietro V, Howard MA, Sanger GJ, Andrews PLR, et al. Functional brain networks and neuroanatomy underpinning nausea severity can predict nausea susceptibility using machine learning. *J Physiol.* (2019) 597:1517–29. doi: 10.1113/JP277474

26. Toschi N, Kim J, Sclocco R, Duggento A, Barbieri R, Kuo B, et al. Motion sickness increases functional connectivity between visual motion and nausea-associated brain regions. *Auton Neurosci.* (2017) 202:108–13. doi: 10.1016/j.autneu.2016.10.003

27. Gavgani AM, Wong RHX, Howe PRC, Hodgson DM, Walker FR, Nalivaiko E. Cybersickness-related changes in brain hemodynamics: a pilot study comparing transcranial Doppler and near-infrared spectroscopy assessments during a virtual ride on a roller coaster. *Physiol Behav.* (2018) 191:56–64. doi: 10.1016/j.physbeh.2018.04.007

28. Hoppes CW, Sparto PJ, Whitney SL, Furman JM, Huppert TJ. Functional near-infrared spectroscopy during optic flow with and without fixation. *PLoS One.* (2018) 13:e0193710. doi: 10.1371/journal.pone.0193710

29. Mishra KP, Yadav AP, Shweta, Chanda S, Majumdar D, Ganju L. Serum levels of immunoglobulins (IgG, IgA, IgM) in Antarctic summer expeditioners and their relationship with seasickness. *Cell Immunol.* (2011) 271:29–35. doi: 10.1016/j.cellimm.2011.05.018

30. Farmer AD, Ban VF, Coen SJ, Sanger GJ, Barker GJ, Gresty MA, et al. Visually induced nausea causes characteristic changes in cerebral, autonomic and endocrine function in humans. *J Physiol.* (2015) 593:1183–96. doi: 10.1113/jphysiol.2014.284240

31. Peddareddygari LR, Kramer PD, Hanna PA, Levenstien MA, Grewal RP. Genetic analysis of a large family with migraine, vertigo, and motion sickness. *Can J Neurol Sci.* (2019) 46:512–7. doi: 10.1017/cjn.2019.64

32. Hromatka BS, Tung JY, Kiefer AK, Do CB, Hinds DA, Eriksson N. Genetic variants associated with motion sickness point to roles for inner ear development, neurological processes and glucose homeostasis. *Hum Mol Genet.* (2015) 24:2700–8. doi: 10.1093/hmg/ddv028

33. Wu Y, Yi F, Akimoto M, Tanaka T, Meng H, Dong Y. Objective measurement and comparison of human facial skin color in East Asian females. *Skin Res Technol.* (2020) 26:584–90. doi: 10.1111/srt.12838

34. Gu HG. [Recording and analysis of EGG and its application in space medicine]. *Space Med Med Eng.* (1999) 12:67–71.

35. Graybiel A, 2nd ME, JL H. Individual differences in susceptibility to motion sickness among six Skylab astronauts. *Acta Astronaut.* (1975) 2:155–74. doi: 10.1016/0094-5765(75)90051-X

36. Ozer ME, Sarica PO, Arga KY. New machine learning applications to accelerate personalized medicine in breast cancer: rise of the support vector machines. *OMICS.* (2020) 24:241–6. doi: 10.1089/omi.2020.0001

37. Zhang C, Ma YQ. *Ensemble Machine Learning: Methods and Applications.* New York, NY: Springer (2012).

38. Arian R, Hariri A, Mehridehnavi A, Fassihi A, Ghasemi F. Protein kinase inhibitors' classification using K-Nearest neighbor algorithm. *Comput Biol Chem.* (2020) 86:107269. doi: 10.1016/j.compbiolchem.2020.107269

39. Lin SK, Hsiu H, Chen HS, Yang CJ. Classification of patients with Alzheimer's disease using the arterial pulse spectrum and a multilayer-perceptron analysis. *Sci Rep.* (2021) 11:8882. doi: 10.1038/s41598-021-87903-7

40. Pedregosa F, Varoquaux G, Gramfort A, Michel V, Thirion B, Grisel O, et al. Scikit-learn: machine learning in python. *J Mach Learn Res.* (2011) 12:2825–30. doi: 10.5555/1953048.2078195

41. Pei JC, Chang L, Liu ZQ, Wang LJ, Li WG, Sun RL. [Selection of vestibular system function in Chinese astronauts]. *Space Med Med Eng.* (2003) 16(Suppl):494–9. doi: 10.16289/j.cnki.1002-0837.2003.s1.008

42. Gruden T, Popovic NB, Stojmenova K, Jakus G, Miljkovic N, Tomazic S, et al. Electrogastrography in autonomous vehicles-an objective method for assessment of motion sickness in simulated driving environments. *Sensors.* (2021) 21:550. doi: 10.3390/s21020550

43. Nobel G, Tribukait A, Mekjavic IB, Eiken O. Effects of motion sickness on thermoregulatory responses in a thermoneutral air environment. *Eur J Appl Physiol.* (2012) 112:1717–23. doi: 10.1007/s00421-011-2142-6

44. Cheung B, Nakashima AM, Hofer KD. Various anti-motion sickness drugs and core body temperature changes. *Aviat Space Environ Med.* (2011) 82:409–15. doi: 10.3357/ASEM.2903.2011

45. Wang L, Cao Y, Tan C, Zhao Q, He S, Niu D, et al. Uncoupling VOR and vestibuloautonomic retention to Coriolis acceleration training in student pilots and control subjects. *J Vestib Res.* (2017) 27:103–12. doi: 10.3233/VES-170608

46. Li Y, Liu A, Ding L. Machine learning assessment of visually induced motion sickness levels based on multiple biosignals. *Biomed Signal Process Control.* (2019) 49:202–11. doi: 10.1016/j.bspc.2018.12.007

47. Li X, Zhu C, Xu C, Zhu J, Li Y, Wu S. VR motion sickness recognition by using EEG rhythm energy ratio based on wavelet packet transform. *Comput Methods Programs Biomed.* (2020) 188:105266. doi: 10.1016/j.cmpb.2019.105266

48. Barmack NH. Central vestibular system: vestibular nuclei and posterior cerebellum. *Brain Res Bull.* (2003) 60:511–41. doi: 10.1016/S0361-9230(03)00055-8

49. Dai M, Raphan T, Cohen B. Labyrinthine lesions and motion sickness susceptibility. *Exp Brain Res.* (2007) 178:477–87. doi: 10.1007/s00221-006-0759-1